Received: 22 September 2023 | Revised: 2 January 2024 | Accepted: 3 January 2024

DOI: 10.1111/epi.17879

Epilepsia®

RESEARCH ARTICLE

Semiautomated electric source imaging determines epileptogenicity of encephaloceles in temporal lobe epilepsy

Dorin-Cristian Antal[1,2,3,4] | **Dirk-Matthias Altenmüller**[1] | **Matthias Dümpelmann**[1] | **Christian Scheiwe**[5] | **Peter C. Reinacher**[6,7] | **Eliza-Theona Crihan**[8] | **Bogdan-Emilian Ignat**[2,4] | **Iulian-Dan Cuciureanu**[3,4] | **Theo Demerath**[9] | **Horst Urbach**[9] | **Andreas Schulze-Bonhage**[1] | **Marcel Heers**[1]

[1]Faculty of Medicine, Epilepsy Center, Medical Center–University of Freiburg, Freiburg, Germany

[2]Neurology Clinic, Rehabilitation Clinical Hospital, Iași, Romania

[3]I Neurology Clinic, "Prof. Dr. N. Oblu" Emergency Clinical Hospital, Iasi, Romania

[4]University of Medicine and Pharmacy "Grigore T. Popa", Iasi, Romania

[5]Department of Neurosurgery, Medical Center–University of Freiburg, Faculty of Medicine, University of Freiburg, Freiburg, Germany

[6]Department of Stereotactic and Functional Neurosurgery, Medical Center–University of Freiburg, Faculty of Medicine, University of Freiburg, Freiburg, Germany

[7]Fraunhofer Institute for Laser Technology, Aachen, Germany

[8]Section II Acute, Institute of Psychiatry "Socola", Iasi, Romania

[9]Department of Neuroradiology, University Hospital Freiburg, Freiburg, Germany

Correspondence
Marcel Heers, Epilepsy Center, Universitätsklinik Freiburg, Breisacher Str. 64, Freiburg D-79106, Germany.
Email: marcel.heers@uniklinik-freiburg.de

Abstract

Objective: We aimed to assess the ability of semiautomated electric source imaging (ESI) from long-term video-electroencephalographic (EEG) monitoring (LTM) to determine the epileptogenicity of temporopolar encephaloceles (TEs) in patients with temporal lobe epilepsy.

Methods: We conducted a retrospective study involving 32 temporal lobe epilepsy patients with TEs as potentially epileptogenic lesions in structural magnetic resonance imaging scans. Findings were validated through invasive intracerebral stereo-EEG in six of 32 patients and postsurgical outcome after tailored resection of the TE in 17 of 32 patients. LTM (mean duration = 6 days) was performed using the 10/20 system with additional T1/T2 for all patients and sphenoidal electrodes in 23 of 32 patients. Semiautomated detection and clustering of interictal epileptiform discharges (IEDs) were carried out to create IED types. ESI was performed on the averages of the two most frequent IED types per patient, utilizing individual head models, and two independent inverse methods (sLORETA [standardized low-resolution brain electromagnetic tomography], MUSIC [multiple signal classification]). ESI maxima concordance and propagation in spatial relation to TEs were quantified for sources with good signal quality (signal-to-noise ratio > 2, explained signal > 60%).

Results: ESI maxima correctly colocalized with a TE in 20 of 32 patients (62.5%) either at the onset or half-rising flank of at least one IED type per patient. ESI maxima showed propagation from the temporal pole to other temporal or extratemporal regions in 14 of 32 patients (44%), confirming propagation originating in the area of the TE. The findings from both inverse methods validated each other in 14 of 20 patients (70%), and sphenoidal electrodes exhibited the highest signal amplitudes in 17 of 23 patients (74%). The concordance of ESI with the TE

predicted a seizure-free postsurgical outcome (Engel I vs. >I) with a diagnostic odds ratio of 2.1.

Significance: Semiautomated ESI from LTM often successfully identifies the epileptogenicity of TEs and the IED onset zone within the area of the TEs. Additionally, it shows potential predictive power for postsurgical outcomes in these patients.

KEYWORDS

electric source imaging, encephalocele, epilepsy surgery, magnetic resonance imaging, temporal lobe epilepsy

1 | INTRODUCTION

Encephaloceles are herniations of brain tissue, typically occurring at the temporal pole in combination with skull defects of the sphenoid bone. They have been identified as a potential cause of temporal lobe epilepsy (TLE), but their epileptogenicity needs further confirmation.[1,2] The true prevalence of temporal encephaloceles (TEs) is likely underestimated. The largest case series to date estimates the prevalence to be between 2% and 4% in general presurgical evaluation of epilepsy patients and up to 10% in drug-resistant TLE patients.[3]

Accurately determining the epileptogenicity of TEs can be challenging, as standard methods in the presurgical evaluation, such as scalp electroencephalography (EEG) and seizure semiology, may not provide sufficient spatial resolution.[4,5] Additionally, 16%–31% of TLE patients are considered nonlesional on routine magnetic resonance imaging (MRI), in contrast to the finding that temporal TEs are often identified in MRIs of patients who were previously reported as having normal results.[6]

Although the temporal pole is a crucial site within temporal lobe seizure networks,[5,7] scalp EEG recordings can barely differentiate between the origins of interictal epileptiform discharges (IEDs) at the sublobar level. IEDs in TLE may exhibit distinct spatiotemporal patterns, but it is nearly impossible to distinguish IEDs of the temporal pole from other regions of the anterior temporal lobe based on scalp EEG traces. Employing either invasive subdural EEG or intracerebral stereo-EEG (iEEG) to adequately cover the temporal pole often involves intricate neurosurgical procedures. As a result, the coverage of the temporal pole with iEEG electrodes is often sparse, sometimes leaving a risk of missing the ictal onset.[8] Consequently, extended iEEG recordings are chosen to determine the epileptogenicity of TEs.[9]

Studying IEDs in scalp EEG recordings offers a noninvasive window for exploration. Compared to seizure onset patterns, IEDs have the advantage of providing high-amplitude, low-noise data. IEDs propagate during their time course at a lobar and sublobar level. The propagation of averaged IED types in scalp EEG from onset to peak can also be confirmed noninvasively.[10] The clinical relevance of IED propagation is evident, as including iEEG contacts that recorded the onset of IEDs in the resection volume is correlated with a favorable postsurgical outcome, similar to the resection of iEEG contacts with high IED rates.[11,12]

Recent advances in IED detection using machine-learning methods have made automated detection software packages available for clinical practice. Utilizing both semiautomated and automated methods for detecting IED types in long-term scalp EEG recordings over multiple days has shown reliable agreement with visually detected IED types and the seizure onset zone.[13] Current automated detection tools can significantly reduce the time required for IED review by identifying IED types, thus making the time-consuming process of visually marking individual IEDs unnecessary, especially when high event counts are needed for electric source imaging (ESI).[14,15]

ESI, based on the latest International Federation of Clinical Neurophysiology 2017 electrode array, is gaining

Key points

- In approximately two thirds of the patients, ESI maxima colocalize with a temporopolar encephalocele
- Propagation from the temporal pole, indicating the IED origin within the encephalocele area, can be shown in nearly half of the patients
- ESI results from the two different inverse methods applied most often validate each other
- Sphenoidal electrodes are highly informative for ESI
- ESI shows promise as a predictor of favorable postsurgical outcomes

prominent interest, as it can provide accurate and reliable clinical information without the need for additional data collection.[16] Recent publications, including a meta-analysis, have shown that ESI performs comparably to other neuroimaging modalities used in presurgical evaluation, reliably localizing IEDs across epilepsy patient populations.[17,18] Several studies have demonstrated that semiautomated ESI accurately localizes the epileptogenic zone.[19–21] ESI based on scalp EEG with 25 electrodes from long-term monitoring (LTM) compares favorably to ESI based on high-density EEG,[20] particularly when clustering single IEDs into IED types that can be averaged to improve their signal-to-noise (SNR) ratio, especially in patients with TLE.[21,22]

Concordance of semiautomated ESI and TEs suggests the epileptogenicity of TEs, which may be suggestive for epilepsy surgery. However, it remains unclear to what extent ESI, based on semiautomatically detected IEDs in LTM using 10/20 EEG electrode coverage with improved coverage of the temporal pole with additional Silverman electrodes (T1/T2) and with or without additional sphenoidal electrodes (low-density EEG with 21–23 electrodes), can contribute to determining the epileptogenicity of TEs in patients with TLE.

We hypothesize that performing ESI on averaged IED types from LTM with low-density EEG, both during the time course of IEDs, will allow us to confirm that these IEDs originate within the TE area. This hypothesis is additionally motivated by prior studies that demonstrated the clinically relevant contribution of sphenoidal electrodes to the accuracy of ESI.[23]

2 | MATERIALS AND METHODS

2.1 | Study design and clinical data

We retrospectively evaluated 32 adult patients with drug-resistant TLE referred for presurgical evaluation to the Epilepsy Center Freiburg between 2010 and 2022. We included all the patients who met the following criteria:

1. Scalp-EEG LTM for longer than 2 days with ictal and interictal recordings.
2. In-house presurgical high-resolution MRI of the head that fulfilled the proposed criteria for presurgical epilepsy diagnostics.[24]
3. TEs with a diameter ≥ 3 mm were the only potentially epileptogenic lesions on MRI.

We excluded patients with prior epilepsy surgery or LTM not done at the Epilepsy Center Freiburg. The study was approved by the institutional ethics board, and all included patients gave their informed consent that their data from presurgical epilepsy diagnostics can be used in research projects.

2.2 | Structural imaging

In each patient, a high-resolution MRI was acquired to detect structural abnormalities of the brain. Computed tomography (CT) of the skull base was performed in a subgroup of patients to assess osseous defects related to the TE. All except two patients underwent 3-T MRI of the brain according to in-house standards of high-resolution epilepsy protocols.[24,25] The remaining two patients had to undergo a similar 1.5-T MRI protocol, as 3-T MRI was contraindicated because of a cardiac pacemaker. We considered all TEs ≥3 mm as potentially epileptogenic lesions. Among other sequences, the epilepsy MRI protocol included three-dimensional MRI sequences with 1-mm isotropic voxels for T1-contrast magnetization prepared rapid gradient echo and fluid-attenuated-inversion recovery sequences and thin-sectioned axial and coronal T2 sequences angulated according to the long axis of the hippocampus. High-resolution CT scans of the skull base (spiral CT or slices with slice thickness <1 mm) were used to confirm the osseous defect corresponding to TEs. The TEs were visually confirmed by an experienced neuroradiologist (H.U.).

2.3 | Long-term monitoring

LTM data with glued scalp EEG electrodes and simultaneous video were acquired for a mean duration of 5.85 days using a Neuvo amplifier (Compumedics Neuroscan). All LTM data were acquired according to the 10/20 system with additional T1/T2 electrodes (Silverman electrodes). Sphenoidal electrodes (Sp1/Sp2) were added in 72% of patients. EEG data had sampling rates between 250 and 1000 Hz. A team of certified and experienced epileptologists (D.-M.A., M.H., A.S.-B.) completed the visual evaluation and marking of IEDs and seizure onsets as part of the presurgical workup.

2.4 | Semiautomated EEG analysis and IED detection

Automated IED detection was performed using Persyst 14c (Persyst). IEDs were detected in electrodes of the 10/20 system and T1/T2 electrodes, but not in sphenoidal electrodes (see Appendix S1 for details).

2.5 | Electric source imaging

For ESI, we created a realistic three-compartment forward model using the software Curry 9 (Compumedics Neuroscan). The source of each IED type was evaluated at the onset, half-rising flank, and peak using the different inverse methods standardized low-resolution brain electromagnetic tomography (sLORETA) and multiple signal classification (MUSIC; Appendix S1 for details).

Propagation of source maxima was quantified between IED type onset, half-rising flank, and peak by Euclidian distance and sublobar parcellation. We only considered sources with high signal quality (SNR > 2, explained signal > 60%) to reduce the risk of analyzing spurious sources.[26] The resulting spatiotemporal evolution of the source maxima per patient was considered as propagation of the specific IED types.

ESI findings and their propagation were classified according to the 17 cortical parcellations of the brain (see also Section 2.7). In addition, we measured the Euclidian distance between ESI findings and the TE. Propagation was considered for distances ≥5 mm, irrespective of the cortical parcel.

2.6 | ESI comparison with iEEG, resection and postsurgical outcome

For seizure onset zone and epileptogenic zone confirmation, respectively, iEEG studies or tailored surgical resections were performed in 18 of 32 patients depending on the concordance of the electroclinical hypothesis and MRI. All patients with doubts about the seizure onset zone in the area of the TE, with bilateral seizure onset zones in scalp EEG, or with bilateral TEs underwent subsequent iEEG. iEEG data were acquired in seven of 32 patients. All seven patients underwent stereo-EEG with unilateral/bilateral implantations that included multiple iEEG electrodes targeting the temporal pole including the TEs, entorhinal cortex, amygdala, anterior hippocampus, parahippocampal gyrus, and basal temporal regions. Surgical resections were performed in 17 of 32 patients according to the consensus of interdisciplinary seizure conferences. A tailored temporal pole resection sparing the mesial temporal structures was chosen in 16 of 17 patients. In one of 17 patient (ID16; Table 1), the amygdala was also included in the resection volume. The resection volume was typically extended 1.5–2.5 cm from the tip of the temporal pole. Postsurgical outcomes were evaluated at least 1 year after surgery based on the Engel classification. In addition to those 17 patients, one patient underwent unilateral temporal pole resection without available postsurgical follow-up. ESI source maxima results were either confirmed by iEEG findings or an Engel class I postsurgical outcome with a follow-up >1 year.

2.7 | Definitions

Concordance between ESI maxima of either one of the two inverse methods and TE was considered if the ESI maxima localized to the temporal pole parcel that contained a TE. We could not differentiate between multiple TEs at the same temporal pole due to a limited spatial resolution of ESI.

We defined the *onset* of an averaged IED as the first 10% of the entire IED, accordingly: either the earliest deflection in the first 7 ms of its rising flank that met the criteria for nonpolyphasic IEDs or the first peak in polyphasic IEDs if the negative amplitude of the highest amplitude of the averaged IED was preceded by an additional amplitude peak (see also Figure 1).[12,27] *Half-rise* was defined as the midpoint between the onset of the rising flank and the maximum negativity of the averaged IED.[12,27]

IED propagation measures the Euclidean distance between the localization of the source maximum at the IED onset and its maximum at the IED peak of the respective inverse method.[12]

Colocalization was referred to as concordance by two distinct inverse methods. Colocalization between the two inverse methods is fulfilled when both inverse methods localize to the temporal pole with a Euclidian distance <2 cm between them.

The cortical surface of each patient was divided into 17 clinically relevant regions of interest.[28,29] The posterior border of the temporal pole was defined by the anterior brainstem and the limen insulae.[30]

2.8 | Statistical analysis

We assessed the relationship between the spatial concordance of ESI maxima and TEs with postsurgical outcomes at the patient level. We defined *true positives* as cases as where ESI of one of the two most frequent IED types per patient spatially matched the temporal pole with a TE (see also Section 2.2).[28] *True negative* refers to cases with no TE at the temporal pole, and no ESI maximum localized to that area. ESI maxima were categorized as *false positive* when an ESI maximum was present at the temporal pole without a TE, and *false negative* when there was no ESI maximum at the temporal pole with a TE.

3 | RESULTS

3.1 | Study population, demographics, and clinical characteristics

We retrospectively included 32 patients (median age = 38.5 years, range = 18–66; median epilepsy duration = 10 years, range = 1–33; 19/32 patients [59.4%]

TABLE 1 Electric source imaging, invasive stereo-EEG, and postsurgical outcome.

ID	TEs on MRI	Colocalization, side	Propagation/electrodes with maximum IED counts	Onset/direction MUSIC	Onset/direction sLORETA	Propagation, mm, MUSIC	Propagation, mm, sLORETA	SP	sEEG (SOZ)	Surgery, outcome, (follow-up, months)
1	1 L	No	No	H/H or A/H	H/H or A/H	%	%	Yes		L TP, IB (46)
2	2 L	No	No	H/H	H/H	%	%	Yes	LT (L TP)	L TP, IA (60)
3	1 R	Yes	No	I/I	C/TP	%	%			
4	1 L, 1 R	Yes, L	No	A/OF	TP/TP	%	%	Yes	BT (B TP)	L TP, IIIA (15)
5	mb	Yes	Yes (O-P), T3	H/H	TP/TP	%	5	Yes		
6	1 R	No	No	ER/ER	C/C	%	%	Yes		R TP, IIB (30)
7	1 L	Yes	Yes (O-P), T1	TP/A	TP/A	13	5			
8	2 L, 1 R	Yes	Yes (O-P), F7	TP/OF	TP/TP	%	5		LT (L TP)	L TP, IA (24)
9	1 R, 2 L	Yes	Yes (O-P), T2	TP/TP	TP/TB	8	20	Yes		
10	2 L	Yes	Yes (O-P), F7	TP/OF	TP/OF	13	13	Yes		
11	1 R	Yes	Yes (H-P), T2/F8	TP/I for both T2 and F8	TP/TP for both T2 and F8	10	%			R TP, IA (60)
12	2 L	Yes	Yes (O-P), F7	TP/OF	TP/OF	30	34	Yes		L TP, IA (12)
13	1 R, 2 L	No	No	OF/OF	OF/OF	%	%	Yes	BT (B TP)	L TP, IIB (36)
14	mb	Yes	No	F7: TP, AT1: I/I	F7: TB/A, T1: TB/TP	%	%	Yes		
15	mb	Yes	No	C/OF	C/TP	%	%	Yes		
16	2 L	No	No	OF/A for both T1 and F7	F7: OF/A, T1: OF/OF	%	%	Yes		L TP + A, IVB (72)
17	mb	No	No	TB/H	C/TB	%	%	Yes		R TP, IC (78)
18	1 L, 1 R	No	No	A/H	A/TB	%	%	Yes		L TP, IB (15)
19	1 L	Yes	Yes (H-P), T1	TP/TP	TP/TP	%	5	Yes		
20	1 R	No	No	OF/A	OF/A	%	%			
21	1 R	No	No	OF/A	TB/TB	%	%	Yes	BT (R TP)	R TP, IVA (48)
22	mb	Yes, L	Yes (O-P), T1/F7	T1: TP/I, F7: I/I	TP/TP for both T1 and F7	25	6	Yes	BT (B TP)	L TP, IB (114)
23	2 L	Yes	No	TP/TP	OF/OF	%	%	Yes		L TP, IA (72)
24	2 L	Yes	Yes (O-P), T1	TP/OF	TP/TP	22	%	Yes		L TP, IIB (12)
25	1 L	No	No	I/OF and A/A	I/OF and A/A	%	%			L TP[a]
26	2 L	No	No	I/H	H/A	%	%	Yes		L TP, IID (36)

(Continues)

TABLE 1 (Continued)

ID	TEs on MRI	Colocalization, side	Propagation/electrodes with maximum IED counts	Onset/direction MUSIC	Onset/direction sLORETA	Propagation, mm, MUSIC	Propagation, mm, sLORETA	SP	sEEG (SOZ)	Surgery, outcome, (follow-up, months)
27	1 L	Yes	Yes (O-P), T1/T3	TP/A	TP/TB	10	14	Yes		L TP, IIA (55)
28	mb	Yes	Yes (O-P), F8	TP/A	ER/TPc	8	%	Yes		
29	mb	Yes	Yes (O-P), T1	TP/ER	TP/A	29	16	Yes		
30	mb	Yes	Yes (O-P), T2	TP/A	TP/A	24	20			
31	mb	No	No	H/C	C/C	%	%			
32	mb	Yes	No	H/TP	TP/TP	%	%			

Abbreviations: %, no propagation; A, amygdala; B, bilateral; C, cortical midline regions; ER, entorhinal cortex; H, hippocampus; H-P, half-rise to peak; I, insula; IED, interictal epileptiform discharge; L, left; mb, multiple bilateral encephaloceles; MRI, magnetic resonance imaging; MUSIC, multiple signal classification; OF, orbitofrontal; O-P, onset to peak; R, right; sEEG, stereoelectroencephalography; sLORETA, standardized low-resolution brain electromagnetic tomography; SOZ, seizure onset zone; SP, sphenoidal electrodes; T: temporal, TB, temporobasal; TE, temporal encephalocele; TP, temporal pole ipsilateral to the encephalocele; TPc, temporal pole contralateral to encephalocele.

[a]No postsurgical follow-up.

males). Their average body mass index (BMI) at LTM was 27.33 kg/m^2, which is in line with more recent findings that an increased BMI of >25 kg/m^2 is a risk factor for TEs.[2] The most frequently reported focal aware seizures were sensory (epigastric or visual) and cognitive (déjà vu).[31]

3.2 | Structural imaging findings

All TEs were located either unilaterally or at both temporal poles within the sphenoid bone. A co-occurring osseous defect was detected in high-resolution CT of the skull base in all patients who underwent CT (15/32 patients [46.8%]). In 17 patients with unilateral TE, 12 TEs were on the left (70.6%) and five TEs were on the right side (29.4%; Figures 2 and 3).

3.3 | Interictal and ictal LTM findings

In clinical evaluation of the LTM, bilateral IEDs were found in both patients with unilateral and patients with bilateral TEs. In patients with unilateral TEs, bilateral IEDs occurred in eight of 17 patients (47%), unilateral IEDs were ipsilateral to the TEs in eight of 17 patients (47%), and IEDs showed contralateral false lateralization in one of 17 patients. In patients with bilateral TEs, eight of 15 patients (53.3%) had bilateral IEDs, and seven of 15 patients (46.7%) had unilateral IEDs on scalp EEG. Ictal scalp EEG was lateralized to the contralateral hemisphere in two patients with unilateral TEs (ID20, ID21), being proven by iEEG studies in one patient.

If sphenoidal electrodes were used, they often showed high signal amplitudes. In 17 of 23 patients with sphenoidal electrodes (74%), they had the highest signal amplitudes at the peak of the averaged IED types.

3.4 | Semiautomated EEG cluster findings

Semiautomated EEG analysis correctly identified IED types in all patients. After selecting the two most frequent IED types per patient, we report a median of 192 IEDs/type (range = 26–522 IEDs/type). Taking into account the individual duration of the LTM, on average 1.5 IEDs/h of these two IED types occurred. Semiautomated clustering identified IED types in 20 of 32 patients (62.5%) on the left side, in five of 32 patients (15.63%) on the right side, in one of 32 patients (3.12%) with false lateralization to the left, and in six of 32 patients (18.75%) bilaterally. In those eight patients with unilateral TE and bilateral IEDs, the highest IED counts

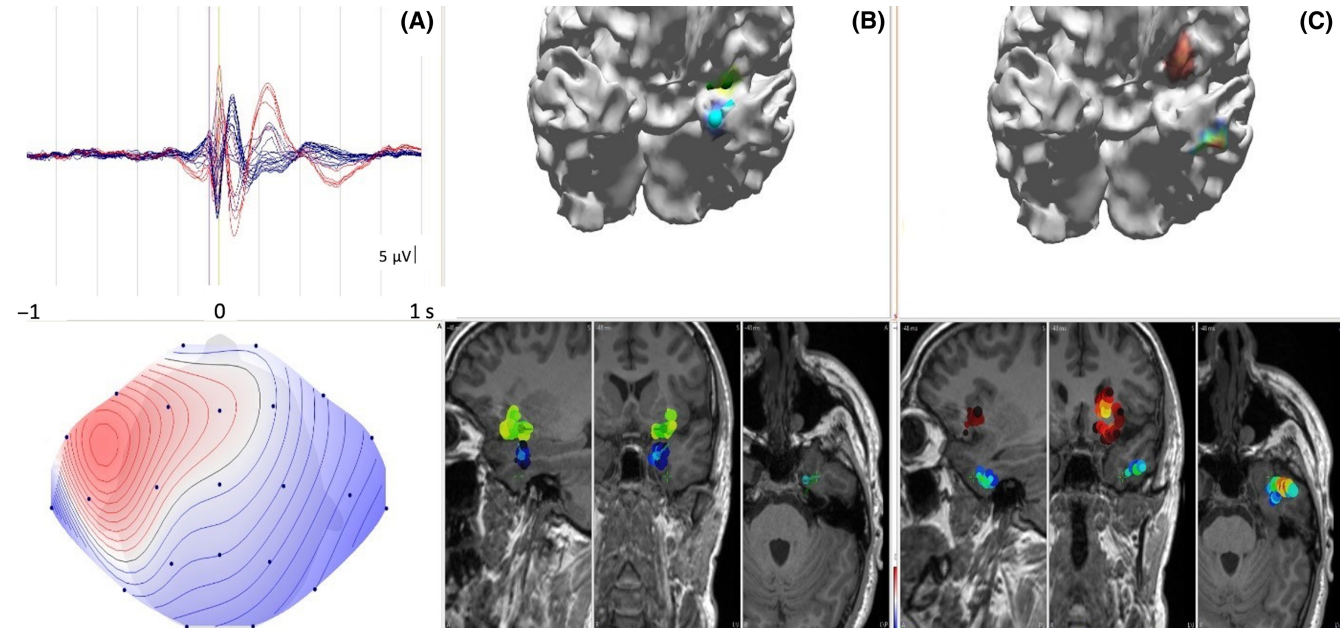

FIGURE 1 Patient ID10 with left-sided temporal lobe epilepsy and multiple unilateral temporopolar encephaloceles. (A) Butterfly plot showing an averaged interictal epileptiform discharge (IED) type and an amplitude map at the onset of the IED type (minor peak in polyphasic IED type). (B) Propagation of the temporopolar blue dipole representing the MUSIC (multiple signal classification) source maximum at the IED onset (color maps thresholded at 95% of the maximum amplitude), adjacent to the temporopolar encephaloceles, to the green dipole localizing to the ipsilateral orbitofrontal cortex at the time of the negative IED maximum. (C) Propagation of the temporopolar sLORETA (standardized low-resolution brain electromagnetic tomography) source maximum in blue at the time of the IED onset (thresholded at 95% of the maximum amplitude), adjacent to the temporopolar encephaloceles, to the red source maximum at the time of the maximum negativity of the IED type. Source maxima of both inverse reconstructions were concordant at the IED onset, and both propagated 13 mm to the ipsilateral orbitofrontal cortex.

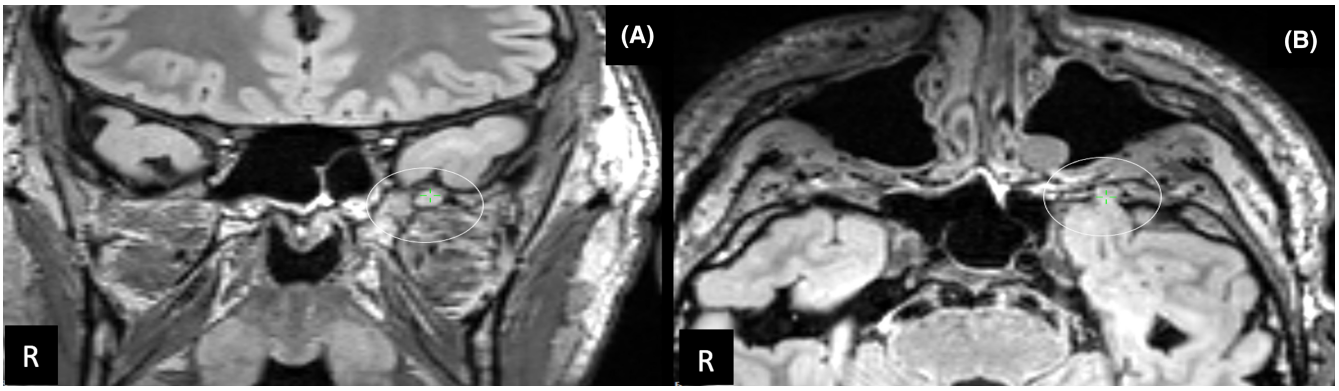

FIGURE 2 Patient ID10. Coronal (A) and axial (B) slices of a three-dimensional fluid attenuated recovery 3-T magnetic resonance imaging sequence of a 19-year-old patient with left temporal lobe epilepsy due to a left temporopolar encephalocele (white circles). R, right.

on semiautomated clustering were always at the side of the TE. All patients with unilateral IEDs in clinical evaluation of LTM had unilateral IED types in semiautomated detection. However, in one patient with right TE, both visually detected IED types in scalp EEG and the most frequent semiautomatically detected IED type localized to the left side (ID20). In the cohort of eight patients with bilateral TEs and bilateral IEDs in clinical evaluation of LTM, the two most frequently detected IED types in semiautomated detection were unilateral in five of eight patients (62.5%).

The highest IED counts were detected for IED types that had their maximum amplitude at the EEG electrodes T1/T2. This was the case in 26 of 32 patients (81.3%), not considering the sphenoidal electrodes Sp1/Sp2, as the detector was not specified to detect IEDs here.

3.5 | ESI findings

The ESI amplitude maximum of at least one inverse method of at least one IED type/patient was concordant with a TE in 20 of 32 patients (62.5%) at the onset, half-rising peak, or peak of the averaged IED type. In patients with unilateral TEs, ESI maxima of at least one inverse method were concordant with the TE in nine of 17 patients (52.9%). In patients with bilateral TEs, 11 of 15 patients (73.3%) were concordant with TEs of at least one side and in two of them with TEs on both sides (see examples in Figures 4 and 5).

Most often, in 14 of 20 patients (70%), source maxima of both inverse methods colocalized with a TE, confirming each other. In the remaining patients, sLORETA was concordant with a TE in four of 20 patients (20%) and MUSIC in two of 20 patients (10%) alone.

IEDs propagated through their time course from a TE to distant regions in a subgroup of patients. IEDs propagated

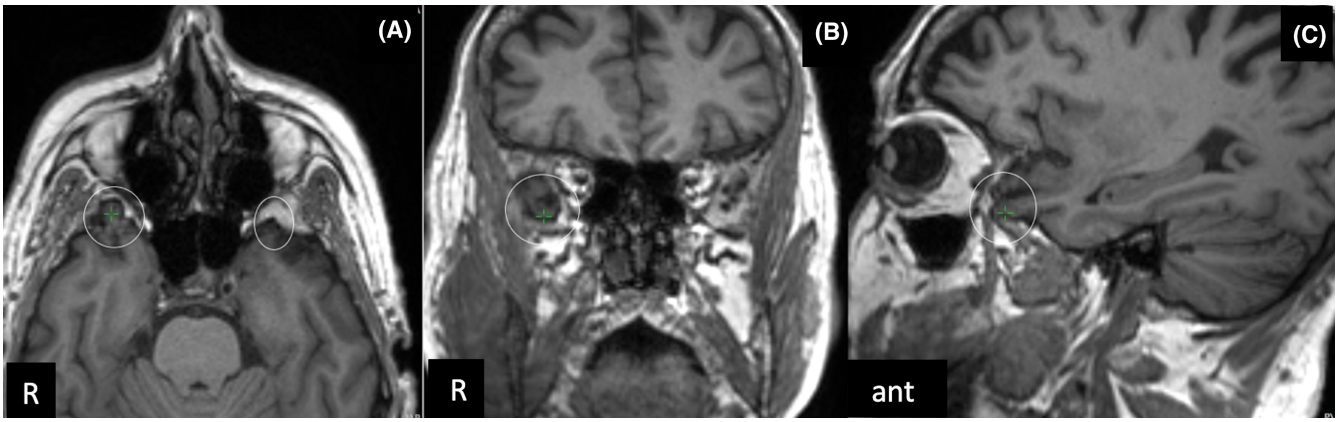

FIGURE 3 Patient ID30. T1 three-dimensional 3-T magnetic resonance imaging sequence of a 65-year-old patient with temporal lobe epilepsy. (A) Axial slices with bilateral (right [R] > left) temporopolar encephaloceles (white circles). (B, C) Coronal (B) and sagittal (C) slices depict two different right temporal encephaloceles close to each other. ant, anterior.

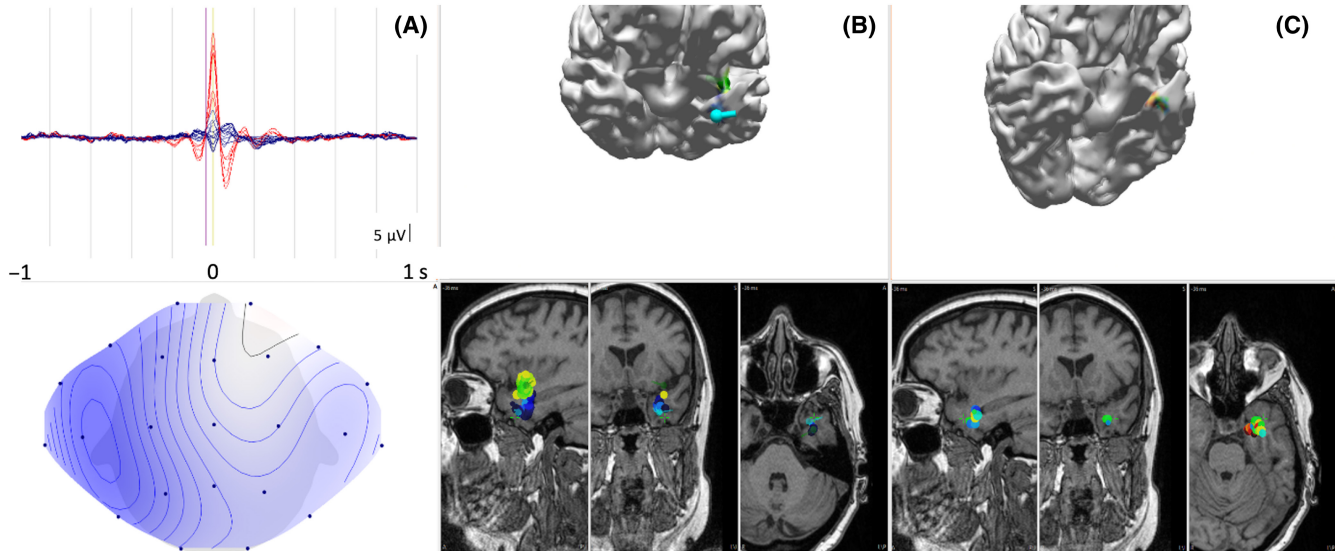

FIGURE 4 Patient ID22 with left temporal lobe epilepsy and bilateral temporopolar encephaloceles. (A) Butterfly plot showing an averaged interictal epileptiform discharge (IED) type and amplitude map at the onset of the IED type. (B) Dipole source maximum of the multiple signal classification (MUSIC) algorithm (color map thresholded at 99% of the maximum amplitude). Propagation is illustrated of the temporopolar blue MUSIC dipole at the onset of the IED type, located near the left-sided temporopolar encephalocele, to the left insular localization of the green dipole at the time of the negative amplitude maximum of the IED type. (C) sLORETA (standardized low-resolution brain electromagnetic tomography) blue source maximum (color map thresholded at 99% of the maximum amplitude) at onset, adjacent to the temporopolar encephalocele, propagated 6 mm within the temporal pole to the red source maximum at the time of the maximum negativity of this IED type. This patient underwent left temporal pole resection after bitemporal intracranial recordings using stereoencephalography and became seizure-free, except for occasional nondisabling focal aware seizures (Engel IB, follow-up for 10 years).

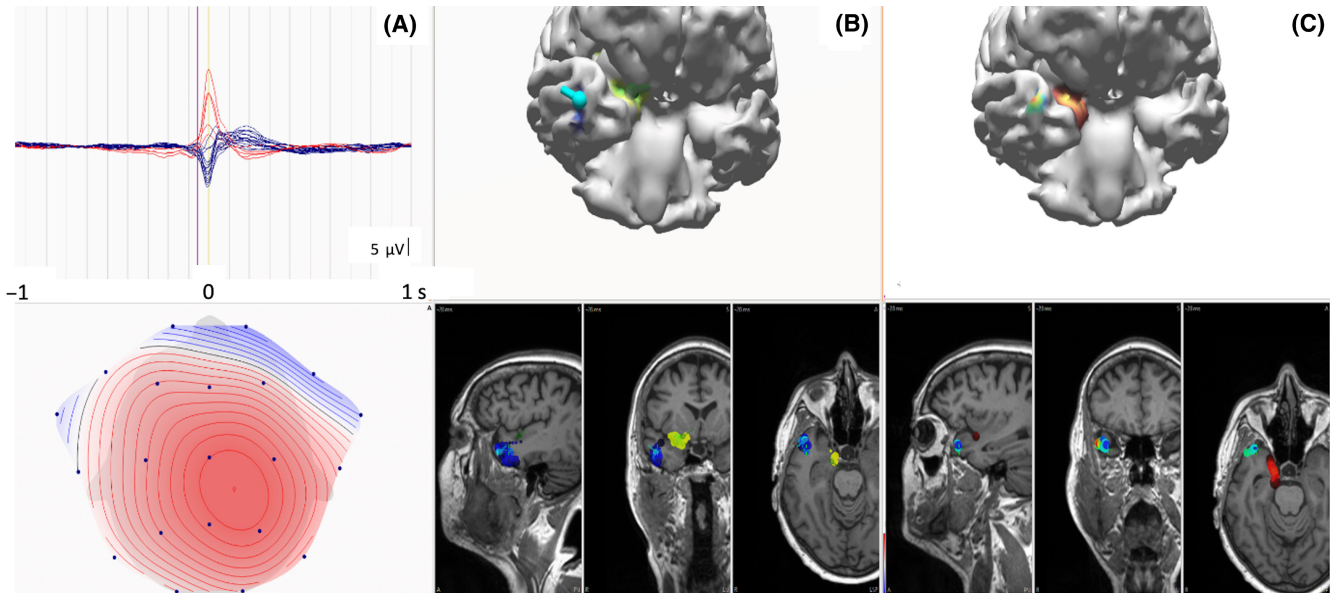

FIGURE 5 Patient ID30 with temporal lobe epilepsy and bilateral temporopolar encephaloceles. (A) Butterfly plot depicting an averaged IED type and amplitude map at the onset of the interictal epileptiform discharge (IED) type. (B) Dipole source maximum of the multiple signal classification (MUSIC) algorithm (color map thresholded at 99% of the maximum amplitude). Propagation is shown of the temporopolar blue MUSIC dipole at the onset of the IED type, adjacent to the right temporopolar encephalocele, to the localization of the green dipole within the ipsilateral amygdala at the time of the negative amplitude maximum of the IED type. (C) Standardized low-resolution brain electromagnetic tomography (sLORETA) source maximum (color maps thresholded at 99% of the maximum). Propagation is shown of the temporopolar sLORETA blue source maximum, adjacent to the temporopolar encephalocele, at the onset of the IED type to the ipsilateral amygdalar location of the red source maximum at the time of the maximum negativity of the IED type. ESI maxima, using either the MUSIC or the sLORETA inverse method, propagated a Euclidean distance of 24 mm and 20 mm, respectively, to the ipsilateral amygdala.

in 14 of 32 patients (44%) by a Euclidian distance of 16 ± 9 mm. Propagation was demonstrated by both inverse methods in eight of 14 patients (57.2%) and in three of 14 patients (21.4%) by either sLORETA or MUSIC, respectively. IEDs propagated to the following regions: amygdala (5/14 [35.7%]), orbitofrontal cortex (3/14 [21.4%]), temporal pole area (3/14 [21.4%]), insula (2/14 [14.3%]), and basal temporal area (1/14 [7.1%]). Propagation was seen between half-rise and peak of the averaged IEDs in two of 14 patients (14.3%) and between onset and peak in 12 of 14 patients (85.7%).

3.6 | Validation by iEEG and postsurgical outcome

From our total cohort, 17 of 32 patients underwent either iEEG or surgical resection with available postsurgical outcome data or both. In six of 32 patients iEEG was acquired, and 17 of 32 patients underwent unilateral temporal pole resection sparing the amygdala and the hippocampus (ID16 was an exception, with resection of the amygdala). In the iEEG subgroup, all six patients had a seizure onset zone in the temporal pole electrodes near the TEs, with accurate colocalization by ESI in four of seven patients (57%). In three of five patients with bilateral iEEG implantation and bilateral TEs, seizures were recorded independently from both temporal poles. Surgery was offered to three of these patients (ID4, ID13, ID21) on the side with the predominant seizures. ESI concurred with the predominant seizure focus. However, although extended lesionectomy of the TE was performed in patients ID4 and ID21, only patient ID4 experienced a favorable postsurgical outcome.

We report Engel I postsurgical outcome at >1 year in nine of 17 surgical patients (52.9%) with a mean follow-up of 53.4 (±31.3) months. In 14 of 17 surgical patients, there was a favorable postsurgical outcome of Engel I/II with a mean follow-up of 46.4 months, seven of 14 (50%) having been correctly colocalized by ESI results. The concordance of ESI with the TE predicts postsurgical outcomes (Engel I vs. >I) with a diagnostic odds ratio of 2.1 (95% confidence interval [CI] = .30–14.55), sensitivity of .63 (95% CI = .37–.84), and specificity of .56 (95% CI = .31–.78), based on data from 17 surgical patients (true positive, 5; false negative, 4; false positive, 3; true negative, 5). We could not establish any relationship between the concordance of ESI maxima and TEs and postsurgical outcomes in patients with multiple bilateral TEs due to an insufficient cohort size. Patients with Engel I outcome did not show a tendency

for a shorter duration of epilepsy compared to patients with Engel outcome II–IV (median = 8/mean = 10.5 years vs. median = 10/mean = 10.4 years), although there was a statistical difference in the comparison of patients with Engel I/II versus III/IV outcome (9.7 ± 31.3 years vs. 14 ± 2.9 years).

4 | DISCUSSION

4.1 | Main findings

ESI maxima of semiautomatically detected IEDs from LTM are often spatially concordant with TEs and can capture propagation from the area of the TE to distant regions throughout the time course of IEDs. ESI maxima during the time course of at least one IED type per patient were spatially concordant with a TE in approximately two thirds of the patients. Spatial concordance between ESI maxima and TE typically occurs for ESI maxima at the onset or at the half-rising flank of the IED type. Secondary propagation from the temporal pole to other temporal or extratemporal regions occurs in almost half of the patients, further supporting the origin of the IED type within the area of the TE. ESI findings of the two different inverse methods applied typically colocalize and thus validate each other. Sphenoidal electrodes are highly informative for ESI, as they most often exhibit the highest signal amplitudes at the peak of the IEDs. ESI can even be considered a predictor of favorable postsurgical outcomes.

4.2 | Spatial concordance

To the best of our knowledge, this study is the first to apply ESI in demonstrating the epileptogenicity of TEs noninvasively. These results underscore the value of concordance between ESI source maxima obtained from LTM and a given TE that may add to presurgical evaluations, as previously reported in more diverse etiologies of focal epilepsies.[11,19] The colocalization of results from different inverse methods enhances confidence in the ESI findings across different patients.[32] Until now, extensive iEEG recordings have been necessary to confirm the epileptogenicity of TEs.[9]

4.3 | Spatiotemporal analysis

The spatiotemporal analysis of ESI maxima at the source level, using IED types based on averaged single IEDs, suggests that IEDs propagate during the time course of the IED. Notably, the first deflection that meets the technical criteria during the onset often spatially corresponds best to the TE, and the IED may propagate with high variability to distant brain regions during the course of the IEDs, such as the amygdala, the hippocampus, and the orbitofrontal cortex. This implies that relying solely on ESI at the peak of the IED type would have led to false localizations distant from the site of the IED onset close to the TE.[10]

The high counts of IEDs per IED type, recorded over multiple days during LTM, provide distinct advantages compared to short-term high-density EEG recordings that typically last only a few hours, and tend to yield relatively few IEDs. Averaging IED types based on semiautomated detection from LTM results in highly accurate ESI findings due to the consistently high SNRs, even at the onset of averaged IED types.[22]

The temporal pole, considered to be a cortical convergence zone with distinct functional and anatomical connections,[33] displays connectivity and propagation patterns distinct from those of mesial temporal structures. It consistently connects with the orbitofrontal area and the inferior frontal gyrus,[34] which may explain the propagation of the ESI maxima to orbitofrontal areas in some of our patients. However, with our current electrode setup, the ESI results of IED propagation need to be interpreted with caution. Although we have high electrode coverage of the temporal pole similar to targeted-density EEG,[35] in areas distant to the temporal pole the electrode coverage is likely suboptimal. Thus, especially source-level IED propagation, for example, to the insula and orbitofrontal cortex, needs to be validated with higher coverage of evenly distributed scalp EEG electrodes with better whole brain coverage.[22]

4.4 | Differentiating between temporopolar and mesial temporal

Unraveling the IED propagation from the TEs to distant brain regions can enhance the distinction between these discharges and those originating from other temporal and extratemporal regions. However, distinguishing mesial temporal lobe IEDs from those of other origins is typically challenging, as mesial temporal IEDs usually need to propagate to the temporal neocortex before they can be distinguished in scalp EEG.[36] There are rare exceptions to this general rule, where even hippocampal epileptic activity can be recognized in scalp EEG.[37] Consequently, our current setup was not optimal to differentiate between temporopolar and mesial temporal sources.

In patients with TLE and TEs, IED types originating clearly in mesial temporal lobe structures could indicate secondary mesial temporal involvement in the course of

the disease and may serve as a predictor for worse postsurgical outcomes. This could be an explanation for the observed tendency toward worse postsurgical outcomes in patients of longer epilepsy duration within our cohort. Fast propagations of evoked potentials from the temporal pole to mesial temporal structures could point toward an increased vulnerability and high risk of secondary epileptogenesis of mesial temporal lobe structures in primarily extrahippocampal TLE.[38]

Simultaneous EEG–functional MRI (fMRI) may be an appropriate method for distinguishing IEDs originating in mesial temporal structures from IEDs originating in the temporal pole. The advantage of EEG-fMRI over ESI lies in its capability to identify the IED onset zone in areas distant from the cortical surface, such as the mesial temporal lobe.[39,40] An alternative approach to characterize the differences between temporopolar and mesial temporal IEDs is simultaneous iEEG/scalp EEG recordings with sufficient noninvasive coverage of the temporal pole.[41]

4.5 | Postsurgical outcome and implementation in clinical practice

The concordance of ESI from LTM with results from presurgical diagnostics demonstrates the potential power to predict favorable postsurgical outcomes, which holds significant clinical relevance. It may support the identification of patients with TEs in whom iEEG studies can be omitted and a very circumscribed temporopolar resection can be offered. Nevertheless, its relatively low sensitivity suggests that it may not be sufficient as a standalone screening tool for detecting potentially epileptogenic TEs.

The presented method introduces a valuable approach with the advantage of high temporal resolution in the presurgical assessment of epilepsy patients. It is important to emphasize that implementing this method relies on readily available EEG and MRI data from presurgical diagnostics. These existing data sources can be combined and processed further to extract additional information. To the best of our knowledge, there is currently no way other than ESI to determine the origin of IEDs in the anterior temporal lobe noninvasively. ESI can probably be useful to determine the epileptogenicity of pathologies of the temporal pole other than TEs as well.

4.6 | Future perspectives

The yield of ESI could likely be enhanced through the utilization of improved head models or alternative scalp EEG setups with comprehensive coverage of the temporal pole. Additionally, the spatial accuracy of ESI might be further improved by employing a more detailed finite element head model and individualized conductivity thresholds.[42] An open question remains regarding the possibility of replacing sphenoidal electrodes with scalp EEG setups that comprehensively cover the temporal pole.[35] It is possible that evenly spaced scalp EEG setups with higher electrode counts and better whole brain coverage could offer more precise tracing of IED propagation paths and aid presurgical evaluations for variable pathologies.

5 | CONCLUSIONS

Semiautomated low-density ESI from LTM with 10/20 electrode coverage, supplemented by T1/T2 and sphenoidal electrodes, is a valuable tool for assessing the epileptogenicity of TEs and studying propagation pathways. Most importantly, it demonstrates promising predictive power for postsurgical outcomes. Therefore, we strongly recommend the integration of ESI based on semiautomatically detected IED types from LTM into clinical practice.

AUTHOR CONTRIBUTIONS

Dorin-Cristian Antal, Marcel Heers, Dirk-Matthias Altenmüller, and Andreas Schulze-Bonhage contributed to the study design and data collection search and selection of studies. Dorin-Cristian Antal, Marcel Heers, and Dirk-Matthias Altenmüller contributed equally to data analysis and interpretation. Matthias Dümpelmann contributed to the interpretation of ESI findings. Theo Demerath and Horst Urbach reviewed MRI findings. Peter C. Reinacher and Christian Scheiwe were responsible for the SEEG and postsurgical monitoring. Dorin-Cristian Antal and Marcel Heers prepared the first draft of the manuscript. Dirk-Matthias Altenmüller, Matthias Dümpelmann, Andreas Schulze-Bonhage, Iulian-Dan Cuciureanu, Eliza-Theona Crihan, Bogdan-Emilian Ignat, Theo Demerath, and Horst Urbach reviewed the manuscript and contributed to its final version. All authors read and approved the final manuscript.

ACKNOWLEDGMENTS

D.-C.A. was a visiting scholar funded by the Michael Foundation at the Epilepsy Center Freiburg in Germany. Open Access funding enabled and organized by Projekt DEAL.

CONFLICT OF INTEREST STATEMENT

None of the authors has any project-related conflict of interest to disclose. We confirm that we have read the Journal's position on issues involved in ethical publication and affirm that this report is consistent with those guidelines.

ORCID

Dorin-Cristian Antal https://orcid.org/0000-0001-8486-1614
Dirk-Matthias Altenmüller https://orcid.org/0000-0001-8610-2216
Matthias Dümpelmann https://orcid.org/0000-0002-1476-7777
Theo Demerath https://orcid.org/0000-0002-5869-1110
Horst Urbach https://orcid.org/0000-0001-7264-4807
Andreas Schulze-Bonhage https://orcid.org/0000-0003-2382-0506
Marcel Heers https://orcid.org/0000-0001-5545-7014

REFERENCES

1. Jagtap SA, Kurwale N, Patil S, Bapat D, Joshi A, Chitnis S, et al. Temporal encephalocele: a rare but treatable cause of temporal lobe epilepsy. Epileptic Disord. 2022;24(6):1073–80. https://doi.org/10.1684/epd.2022.1487
2. Urbach H, Jamneala G, Mader I, Egger K, Yang S, Altenmüller D. Temporal lobe epilepsy due to meningoencephaloceles into the greater sphenoid wing: a consequence of idiopathic intracranial hypertension? Neuroradiology. 2018;60(1):51–60. https://doi.org/10.1007/s00234-017-1929-5
3. Saavalainen T, Jutila L, Mervaala E, Kälviäinen R, Vanninen R, Immonen A. Temporal anteroinferior encephalocele: An underrecognized etiology of temporal lobe epilepsy? Neurology. 2015;85(17):1467–74. https://doi.org/10.1212/wnl.0000000000002062
4. Saute RL, Peixoto-Santos JE, Velasco TR, Leite JP. Improving surgical outcome with electric source imaging and high field magnetic resonance imaging. Seizure. 2021;90:145–54. https://doi.org/10.1016/j.seizure.2021.02.006
5. Chabardès S, Kahane P, Minotti L, Tassi L, Grand S, Hoffmann D, et al. The temporopolar cortex plays a pivotal role in temporal lobe seizures. Brain. 2005;128(Pt 8):1818–31. https://doi.org/10.1093/brain/awh512
6. Nguyen DK, Mbacfou MT, Nguyen DB, Lassonde M. Prevalence of nonlesional focal epilepsy in an adult epilepsy clinic. Can J Neurol Sci. 2013;40(2):198–202. https://doi.org/10.1017/s0317167100013731
7. Abel TJ, Woodroffe RW, Nourski KV, Moritani T, Capizzano AA, Kirby P, et al. Role of the temporal pole in temporal lobe epilepsy seizure networks: an intracranial electrode investigation. J Neurosurg. 2018;129(1):165–73. https://doi.org/10.3171/2017.3.JNS162821
8. Abel TJ, Rhone AE, Nourski KV, Granner MA, Oya H, Griffiths TD, et al. Mapping the temporal pole with a specialized electrode array: technique and preliminary results. Physiol Meas. 2014;35(3):323–37. https://doi.org/10.1088/0967-3334/35/3/323
9. Panov F, Li Y, Chang EF, Knowlton R, Cornes SB. Epilepsy with temporal encephalocele: characteristics of electrocorticography and surgical outcome. Epilepsia. 2016;57(2):e33–8. https://doi.org/10.1111/epi.13271
10. Mălîia MD, Meritam P, Scherg M, Fabricius M, Rubboli G, Mîndruţă I, et al. Epileptiform discharge propagation: analyzing spikes from the onset to the peak. Clin Neurophysiol. 2016;127(4):2127–33. https://doi.org/10.1016/j.clinph.2015.12.021
11. Azeem A, von Ellenrieder N, Hall J, Dubeau F, Frauscher B, Gotman J. Interictal spike networks predict surgical outcome in patients with drug-resistant focal epilepsy. Ann Clin Transl Neurol. 2021;8(6):1212–23. https://doi.org/10.1002/acn3.51337
12. Matarrese MAG, Loppini A, Fabbri L, Tamilia E, Perry MS, Madsen JR, et al. Spike propagation mapping reveals effective connectivity and predicts surgical outcome in epilepsy. Brain. 2023;146:3898–912. https://doi.org/10.1093/brain/awad118
13. Heers M, Böttcher S, Kalina A, Katletz S, Altenmüller D-M, Baroumand AG, et al. Detection of interictal epileptiform discharges in an extended scalp EEG array and high-density EEG-A prospective multicenter study. Epilepsia. 2022;63(7):1619–29. http://dx.doi.org/10.1111/epi.17246
14. Scherg M, Ille N, Weckesser D, Ebert A, Ostendorf A, Boppel T, et al. Fast evaluation of interictal spikes in long-term EEG by hyper-clustering: fast evaluation of Interictal spikes. Epilepsia. 2012;53(7):1196–204. https://doi.org/10.1111/j.1528-1167.2012.03503.x
15. Reus EEM, Visser GH, Cox FME. Using sampled visual EEG review in combination with automated detection software at the EMU. Seizure. 2020;80:96–9. https://doi.org/10.1016/j.seizure.2020.06.002
16. Foged MT, Martens T, Pinborg LH, Hamrouni N, Litman M, Rubboli G, et al. Diagnostic added value of electrical source imaging in presurgical evaluation of patients with epilepsy: a prospective study. Clin Neurophysiol. 2020;131(1):324–9. https://doi.org/10.1016/j.clinph.2019.07.031
17. Sharma P, Scherg M, Pinborg LH, Fabricius M, Rubboli G, Pedersen B, et al. Ictal and interictal electric source imaging in pre-surgical evaluation: a prospective study. Eur J Neurol. 2018;25(9):1154–60. https://doi.org/10.1111/ene.13676
18. Sharma P, Seeck M, Beniczky S. Accuracy of interictal and ictal electric and magnetic source imaging: a systematic review and meta-analysis. Front Neurol. 2019;10:1250. https://doi.org/10.3389/fneur.2019.01250
19. Baroumand AG, van Mierlo P, Strobbe G, Pinborg LH, Fabricius M, Rubboli G, et al. Automated EEG source imaging: a retrospective, blinded clinical validation study. Clin Neurophysiol. 2018;129(11):2403–10. https://doi.org/10.1016/j.clinph.2018.09.015
20. Vorderwülbecke BJ, Baroumand AG, Spinelli L, Seeck M, van Mierlo P, Vulliémoz S. Automated interictal source localisation based on high-density EEG. Seizure. 2021;92:244–51. https://doi.org/10.1016/j.seizure.2021.09.020
21. Coito A, Biethahn S, Tepperberg J, Carboni M, Roelcke U, Seeck M, et al. Interictal epileptogenic zone localization in patients with focal epilepsy using electric source imaging and directed functional connectivity from low-density EEG. Epilepsia Open. 2019;4(2):281–92. https://doi.org/10.1002/epi4.12318
22. Spinelli L, Baroumand AG, Vulliemoz S, Momjian S, Strobbe G, van Mierlo P, et al. Semiautomatic interictal electric source localization based on long-term electroencephalographic monitoring: a prospective study. Epilepsia. 2023;64(4):951–61. https://doi.org/10.1111/epi.17460
23. Hamaneh MB, Limotai C, Lüders HO. Sphenoidal electrodes significantly change the results of source localization of

interictal spikes for a large percentage of patients with temporal lobe epilepsy. J Clin Neurophysiol. 2011;28(4):373–9. https://doi.org/10.1097/WNP.0b013e3182273225
24. Wellmer J, Quesada CM, Rothe L, Elger CE, Bien CG, Urbach H. Proposal for a magnetic resonance imaging protocol for the detection of epileptogenic lesions at early outpatient stages. Epilepsia. 2013;54(11):1977–87. https://doi.org/10.1111/epi.12375
25. Urbach H, Scheiwe C, Shah MJ, Nakagawa JM, Heers M, San Antonio-Arce MV, et al. Diagnostic accuracy of epilepsy-dedicated MRI with post-processing. Clin Neuroradiol. 2023;33:709–19. https://doi.org/10.1007/s00062-023-01265-3
26. Whittingstall K, Stroink G, Gates L, Connolly JF, Finley A. Effects of dipole position, orientation and noise on the accuracy of EEG source localization. Biomed. Eng. 2003;2:14. https://doi.org/10.1186/1475-925x-2-14
27. Satzer D, Esengul YT, Warnke PC, Issa NP, Nordli DR Jr. SEEG in 3D: Interictal source localization from intracerebral recordings. Front Neurol. 2022;13:782880. https://doi.org/10.3389/fneur.2022.782880
28. Heers M, Chowdhury RA, Hedrich T, Dubeau F, Hall JA, Lina J-M, et al. Localization accuracy of distributed inverse solutions for electric and magnetic source imaging of interictal epileptic discharges in patients with focal epilepsy. Brain Topogr. 2016;29(1):162–81. https://doi.org/10.1007/s10548-014-03-1
29. Chabardès S, Kahane P, Minotti L, Hoffmann D, Benabid A-L, editors. Anatomy of the temporal pole region. Epileptic Disord. 2002;4(1):S9–S15.
30. Demerath T, Donkels C, Reisert M, Heers M, Rau A, Schröter N, et al. Gray-white matter blurring of the temporal pole associated with hippocampal sclerosis: a microstructural study involving 3 T MRI and ultrastructural histopathology. Cereb Cortex. 2022;32(9):1882–93. https://doi.org/10.1093/cercor/bhab320
31. Fisher RS, Cross JH, French JA, Higurashi N, Hirsch E, Jansen FE, et al. Operational classification of seizure types by the international league against epilepsy: position paper of the ILAE Commission for Classification and Terminology. Epilepsia. 2017;58(4):522–30. https://doi.org/10.1111/epi.13670
32. de Gooijer-van de Groep KL, Leijten FSS, Ferrier CH, Huiskamp GJM. Inverse modeling in magnetic source imaging: comparison of MUSIC, SAM(g2), and sLORETA to interictal intracranial EEG: MEG evaluation in epilepsy. Hum Brain Mapp. 2013;34(9):2032–44. https://doi.org/10.1002/hbm.22049
33. Pascual B, Masdeu JC, Hollenbeck M, Makris N, Insausti R, Ding S-L, et al. Large-scale brain networks of the human left temporal pole: a functional connectivity MRI study. Cereb Cortex. 2015;25(3):680–702. https://doi.org/10.1093/cercor/bht260
34. Papinutto N, Galantucci S, Mandelli ML, Gesierich B, Jovicich J, Caverzasi E, et al. Structural connectivity of the human anterior temporal lobe: a diffusion magnetic resonance imaging study: structural connectivity of the human ATL: a DTI study. Hum Brain Mapp. 2016;37(6):2210–22. https://doi.org/10.1002/hbm.23167
35. Horrillo-Maysonnial A, Avigdor T, Abdallah C, Mansilla D, Thomas J, von Ellenrieder N, et al. Targeted density electrode placement achieves high concordance with traditional high-density EEG for electrical source imaging in epilepsy. Clin Neurophysiol. 2023;156:262–71. https://doi.org/10.1016/j.clinph.2023.08.009
36. Zumsteg D, Friedman A, Wieser HG, Wennberg RA. Source localization of interictal epileptiform discharges: comparison of three different techniques to improve signal to noise ratio. Clin Neurophysiol. 2006;117(3):562–71. https://doi.org/10.1016/j.clinph.2005.11.014
37. Heers M, Reinacher PC, Scheiwe C, Schulze-Bonhage A, Altenmüller D-M. Distinct ictal hippocampal sharp transients in scalp EEG. Clin Neurophysiol. 2020;131(8):1925–7. https://doi.org/10.1016/j.clinph.2020.05.012
38. Novitskaya Y, Dümpelmann M, Vlachos A, Reinacher PC, Schulze-Bonhage A. In vivo-assessment of the human temporal network: evidence for asymmetrical effective connectivity. Neuroimage. 2020;1(214):116769. https://doi.org/10.1016/j.neuroimage.2020.116769
39. Khoo HM, von Ellenrieder N, Zazubovits N, He D, Dubeau F, Gotman J. The spike onset zone: the region where epileptic spikes start and from where they propagate. Neurology. 2018;91(7):e666–74. https://doi.org/10.1212/wnl.0000000000005998
40. Heers M, Hedrich T, An D, Dubeau F, Gotman J, Grova C, et al. Spatial correlation of hemodynamic changes related to interictal epileptic discharges with electric and magnetic source imaging: BOLD and source imaging in epilepsy. Hum Brain Mapp. 2014;35(9):4396–414. https://doi.org/10.1002/hbm.22482
41. Koessler L, Cecchin T, Colnat-Coulbois S, Vignal J-P, Jonas J, Vespignani H, et al. Catching the invisible: mesial temporal source contribution to simultaneous EEG and SEEG recordings. Brain Topogr. 2015;28(1):5–20. https://doi.org/10.1007/s10548-014-0417-z
42. Unnwongse K, Rampp S, Wehner T, Kowoll A, Parpaley Y, von Lehe M, et al. Validating EEG source imaging using intracranial electrical stimulation. Brain Commun. 2023;5:fcad023. https://doi.org/10.1093/braincomms/fcad023

SUPPORTING INFORMATION

Additional supporting information can be found online in the Supporting Information section at the end of this article.

How to cite this article: Antal D-C, Altenmüller D-M, Dümpelmann M, Scheiwe C, Reinacher PC, Crihan E-T, et al. Semiautomated electric source imaging determines epileptogenicity of encephaloceles in temporal lobe epilepsy. Epilepsia. 2024;65:651–663. https://doi.org/10.1111/epi.17879